

# Fast Calculation of the Response of an ECT Probe in the Presence of a Crack

Yann LE BIHAN, Claude MARCHAND, Laboratoire de Génie Electrique de Paris, CNRS  
– Supélec – UPS – UPMC, Gif-sur-Yvette Cedex, France

József PÁVÓ, Department of Broadband Infocommunications and Electromagnetic Theory,  
Budapest University of Technology and Economics, Budapest, Hungary

**Abstract.** A method is presented for the calculation of the interaction of an eddy current testing probe with cracks in a plate. The method is obtained by combining the boundary integral (BIM) and finite element (FEM) methods preserving their attractive properties, that is, the fast and accurate evaluation of the defect field and the versatility in specimen and probe geometry, respectively. FEM is applied for the computation of the electric field induced in the specimen without cracks. Using this, the BIM provides the field perturbation due to the presence of the cracks in the specimen. The good agreement between measured and simulated probe responses shows the applicability of the presented method.

## 1. Introduction

The improvement of the numerical simulation tools contributes to the improvement of the performance of eddy current testing (ECT) by allowing the design of dedicated probes. Within this context, the modelling of the probe-flaw interaction is of great interest. The probe signal due to a crack in a conducting plate is usually calculated by using either integral or variational methods [1-6]. Both methods have their advantages and disadvantages. The finite element method (FEM) is flexible in specimen and probe geometry, while it might require very dense discretization at the vicinity of the crack. In the same time signal calculated in different probe positions are calculated independently, so the evaluation of a scan by FEM is time consuming. In the case of boundary integral method (BIM) only the crack (that is actually assumed as an infinitesimally thin surface) is discretized. The calculations related to different probe positions result in the same system matrix, consequently the evaluation of the signal related to the different probe positions is very fast once the system matrix is established. The difficulties with the BIM are the lack of flexibility in specimen and probe geometry.

An interesting type of ECT signal calculation methods can be formed from the combination of BIM and FEM preserving their attractive properties that is the fast evaluation of the defect field and the versatility in specimen and probe geometry, respectively. In this paper we report the results of a FEM-BIM combination method developed for the calculation of the crack signal. In this approach the incident field due to the interaction of the probe and the crack-free specimen is calculated by FEM and the signal variation due to the presence of the crack is analysed by BIM.

In the following first the investigated arrangements are shown then the analysis method is discussed, finally obtained theoretical results are compared with experimental data.

## 2. Investigated Arrangements

The FEM-BIM combination was implemented for two kinds of ECT probes. The first one is an U-shaped core probe (see Fig. 1) and the second one is a stick core probe (see Fig. 2). The U-core probe is fitting to the detection of cracks oriented parallel to the axis formed by the two poles of the core whereas the stick probe has an isotropic sensitivity. The conductivity and the thickness of the investigated non-magnetic planar specimen are 0.76 MS/m and 3 mm, respectively. Several rectangular EDM (electric discharge machining) notches of different sizes were manufactured in this specimen. Each notch has a 100  $\mu\text{m}$  opening. Their length and depth are both smaller than 1 mm.

The U-core probe is made of a pair of coils wound around the poles of an U-shaped ferrite core. The coils are serially connected in such a way that the generated magnetic field is oriented from one pole to the other and it is approximately uniform between the poles. The pole cross-section is 1 mm  $\times$  1 mm, its height is 1 mm and the pole air-gap is 1 mm. The coil height is 1 mm and the coil cross-section is 1 mm  $\times$  0.45 mm. The number of turns of one coil is 202.

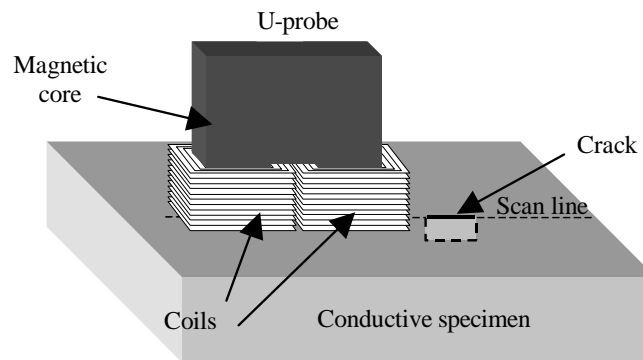


**Fig. 1.** U-core probe

The stick-core probe has an axial symmetry. It is made of a pancake coil wound around a ferrite stick core (see Fig. 2). The radius of the core is 0.4 mm and its height is 4 mm. The external radius and the length of the coil are 0.6 mm and 1.2 mm, respectively.

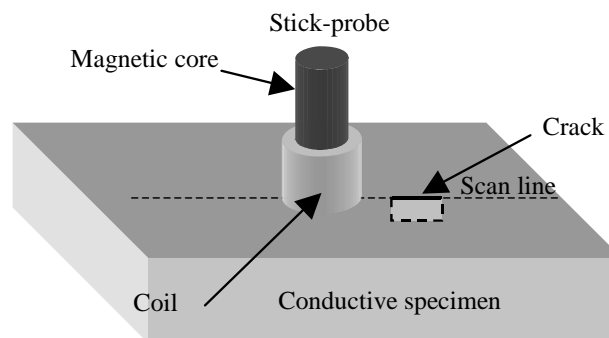


**Fig. 2.** Stick-core probe

The modelling of the U-probe implies 3D FEM meshing whereas only 2D-axisymmetric meshing is needed for the analysis of the stick-probe since the FEM calculation is done in the absence of flaws. The results of the hybrid calculation were compared with experimental ones. For the experimentation the probes were moved with a PC-controlled

robot and the impedance is measured using a 4192A low frequency impedance analyser (Fig. 3). No procedure aiming to calibrate the data was carried out on the impedance measurement results (in particular no calibration flaws are used).

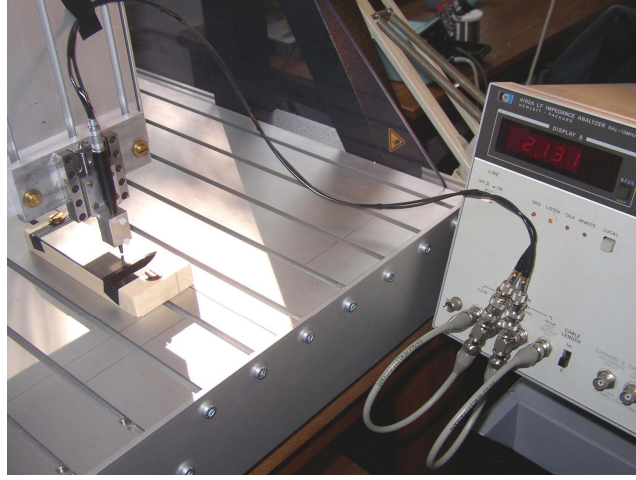


**Fig. 3.** Experimentation system

### 3. Crack signal computation

#### 3.1. Calculation of the probe signal by BIM

The normal component of the current density and hence of the electric field must be zero on the surface  $\Gamma$  representing the crack [3]. This boundary condition can be satisfied by placing on this surface a current dipole distribution (a secondary source) having a normal component only so that it has the same effect as the presence of the crack. In other words, on the surface of the crack the normal component of the current density caused by the current dipoles is the same that is caused by the exciting coil in the absence of the crack but with opposite sign. The sum of the electric field generated by the exciting coil and the secondary source in the homogeneous conductor will provide the field generated by the crack-probe interaction. This consideration leads to the integral equation [3]:

$$0 = E_n^i(\mathbf{r}_0) + \lim_{r \rightarrow r_0} \left[ -j\omega\mu \int_{\Gamma} G^{mn}(\mathbf{r} | \mathbf{r}') p(\mathbf{r}') d\mathbf{r}' \right]; \quad \mathbf{r}_0 \in \Gamma \quad (1)$$

where  $p(\mathbf{r})$  is the normal component of the unknown current dipole density function,  $\omega$  is the angular frequency of the exciting current and  $\mu$  is the conductor permeability.  $G^{mn}$  is the element of the Green's dyad which transforms the normal component of the current dipole density into the normal component of the electric field.  $E_n^i$  represents the normal component of the electric field generated by the exciting coil in the homogeneous plate obtained from the FEM. The numerical solution of (1) yields  $p(\mathbf{r})$ . This solution necessitates the discretization of  $\Gamma$  only, therefore, the number of unknowns is low. Having the solution,  $p(\mathbf{r})$ , and knowing  $E_n^i$ , one can easily calculate the impedance variation,  $\Delta Z$ , of the probe due to the presence of the crack using the reciprocity theory [3]:

$$I^2 \Delta Z = - \int_{\Gamma} E_n^i(\mathbf{r}) p(\mathbf{r}) d\mathbf{r} \quad (2)$$

where  $I$  is the current feeding the probe.

### 3.2. Finite element computation to calculate the incident field

The FEM allows to calculate the incident electric field (i.e. the field in absence of defect) in the crack-free specimen taking into account the characteristics of the probe. For an axisymmetric probe, such as the stick probe, an axisymmetric formulation using for example the magnetic vector potential ( $A$ ) can be used. The nodal degrees of freedom are constituted by the product of  $A$  with the node radial coordinate. The U-core probe as for it involves a 3D modelling. Nevertheless thanks to the symmetry and antisymmetry planes of the probe-specimen configuration in absence of defect, only a quarter of the problem required to be meshed (Fig. 4). An edge-nodal potential formulation combining the magnetic vector and the electric scalar potentials as degrees of freedom was used for this FEM computation [5].

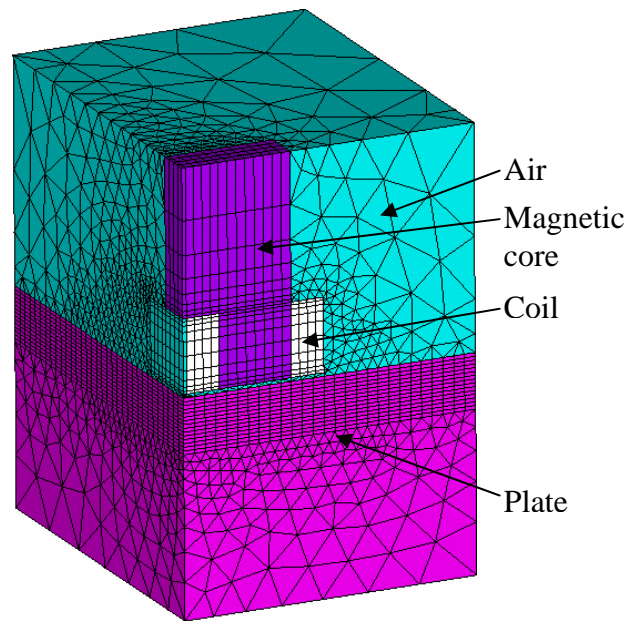


**Fig. 4.** Mesh of the U-core probe

It must be noticed that the FEM calculation is done in the absence of the flaw, so the spatial variation of the electric field in the specimen is described by a relatively smooth function. As a consequence, while accurate results are required the meshing and other aspects of the FEM calculations are not particularly difficult tasks. The mesh of the FEM calculation is chosen independently from the BIM discretization. Once the incident field is deduced from the FEM degree of freedoms, it is interpolated in order to match the BIM discretization. The impedance of the probe in absence of crack is also deduced from the FEM computation by calculating the power loss in the specimen and the magnetic energy in the whole meshed space.

## 4. Comparison between experimental and calculation results

### 4.1. Results obtained with the U-core probe

Figs. 5 and 6 show the comparison between calculated and computed signals for two notch sizes with a scan according to the line defined in Fig. 1. The frequency of the excitation was 800 kHz in this experiment.

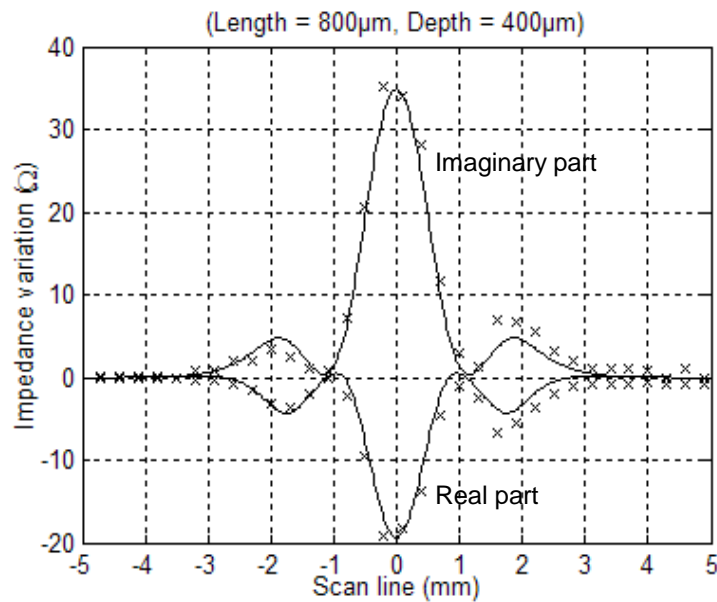


**Fig. 5.** U-probe: calculation (-) and experimental (x) results for a 800  $\mu\text{m}$  (length)  $\times$  400  $\mu\text{m}$  (depth) notch

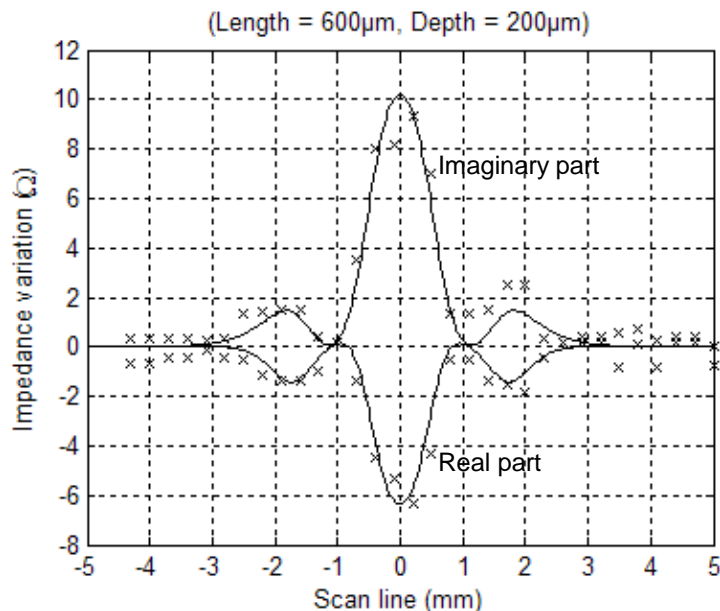


**Fig. 6.** U-probe: calculation (-) and experimental (x) results for a 600  $\mu\text{m}$  (length)  $\times$  200  $\mu\text{m}$  (depth) notch

The small size of the stick-probe allows the detection of smaller flaws. Figs. 7 and 8 show the comparison between calculated and computed signals for two minute notches along the scan line defined in Fig. 2. The frequency of the excitation was 2 MHz in this experiment.

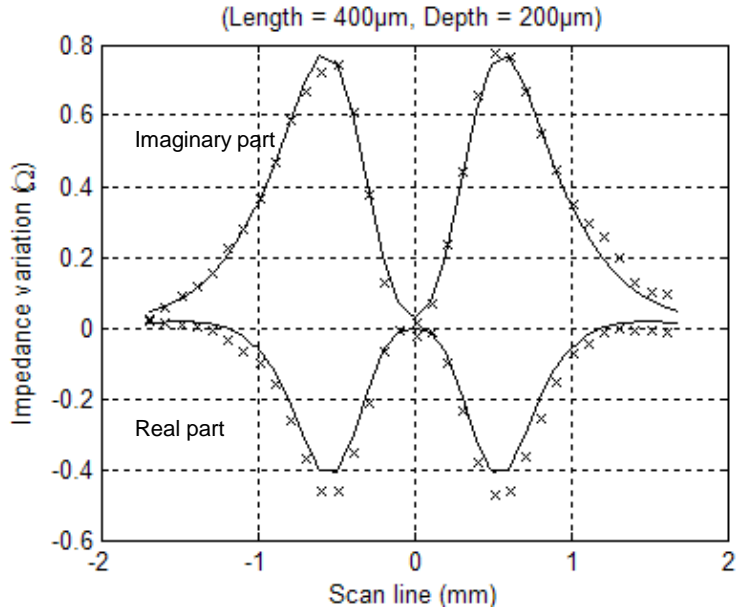


**Fig. 7.** Stick-probe: calculation (-) and experimental (x) results for a 400  $\mu\text{m}$  (length)  $\times$  200  $\mu\text{m}$  (depth) notch

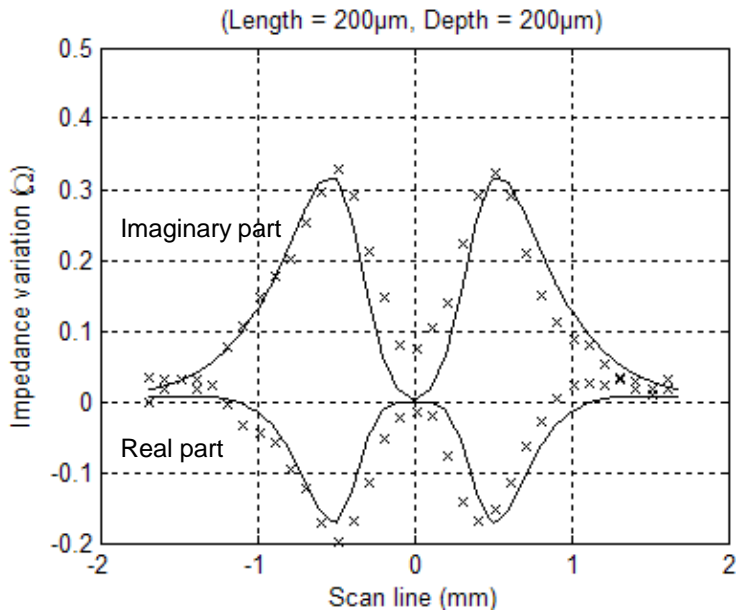


**Fig. 8.** Stick-probe: calculation (-) and experimental (x) results for a 200  $\mu\text{m}$  (length)  $\times$  200  $\mu\text{m}$  (depth) notch

For both probes and for the different notches considered, good agreement is obtained between calculation and experimentation. Note that for such small size flaws there are several possible sources of significant discrepancy between calculation and experimentation, such as for example: uncertainties on the real shape and size of the notches, mechanical and electronic noises, etc. It must be also noticed that these results are obtained even if the experimental notches have an opening that is not negligible compared to their length and depth while the numerical model considers zero thickness crack.

As an example and also to examine the obtained agreement on 2D-scans, Figs. 9 and 10 show experimental and calculated 2D-scans obtained with the U-core probe and the stick-core probe, respectively.



800  $\mu\text{m}$  (length)  $\times$  400  $\mu\text{m}$  (depth)

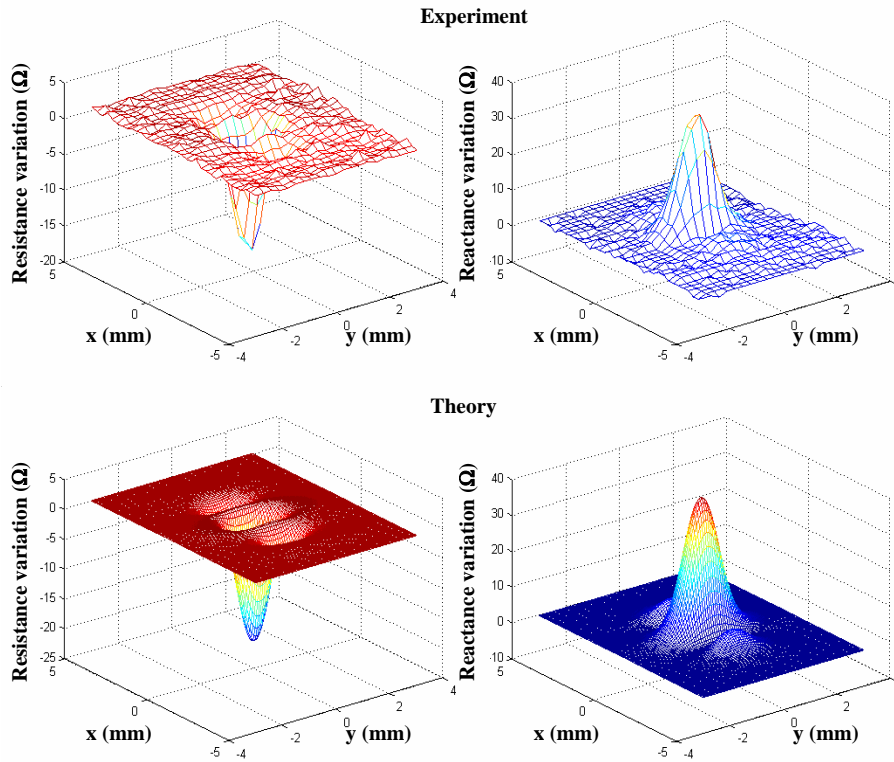


Fig. 9. U-probe: calculation and experimental 2D-scan for a 800  $\mu\text{m}$  (length)  $\times$  400  $\mu\text{m}$  (depth) notch

400  $\mu\text{m}$  (length)  $\times$  200  $\mu\text{m}$  (depth)

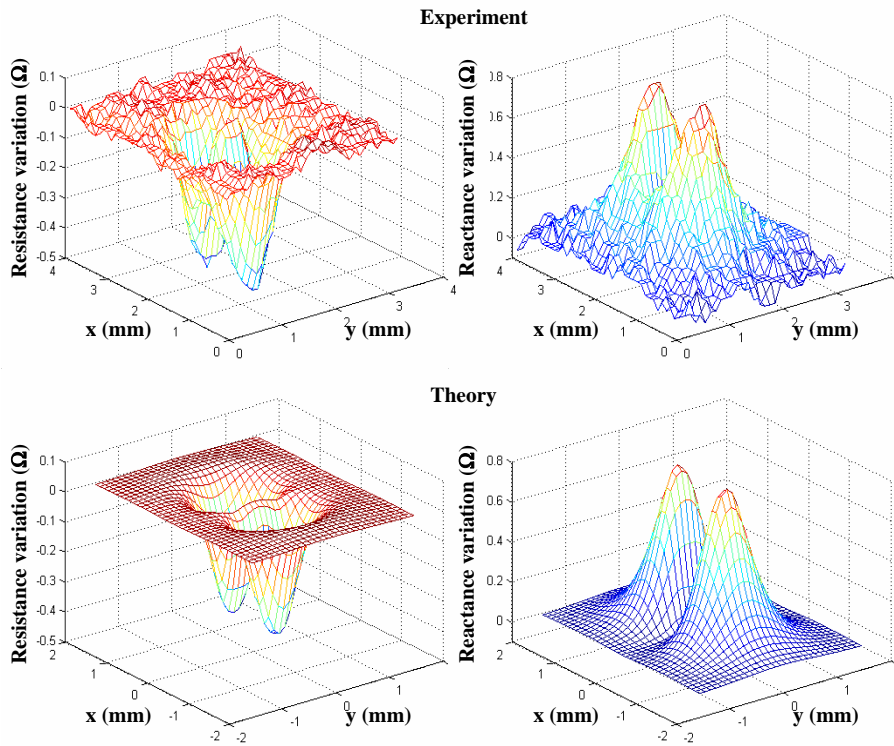


Fig. 10. Stick-probe: calculation and experimental 2D-scan for a 400  $\mu\text{m}$  (length)  $\times$  200  $\mu\text{m}$  (depth) notch

## 5. Conclusion

The good agreement between the measurements and the calculations supports the validity of the numerical model and the applicability of the combination method for the prediction of the signal induced by the interaction of ECT probes and cracks. Using the developed tool the computational requirements of complex problems are significantly decreased making it possible to target probe design and inverse problems meeting the requirements of advanced ECT industry.

## Acknowledgements

This work was technically supported by the engine manufacturer Snecma.

## References

- [1] N. Ida, Numerical Modeling for Electromagnetic Non-Destructive Evaluation, Chapman & Hall, London, 1995.
- [2] B.A. Auld, J.C.Moulder, Review of advances in quantitative eddy current nondestructive evaluation, *J of Nondestructive Evaluation* 1999; 18(1): 3-36.
- [3] J.R. Bowler, Eddy current interaction with ideal crack, Part I: the forward problem, *J. of Applied Physics* 1994; 75(12): 8128-8137.
- [4] J. Pavo, K.Miya, Reconstruction of crack shape by optimization using eddy current field measurement, *IEEE Trans. Magn.* 1994; 30(5): 3407-3410.
- [5] Z. Ren, A. Razek, Computation of 3-D electromagnetic field using differential forms based elements and dual formulations, *Int. J. of Numerical Modelling: Electronic Networks, Devices and Fields* 1996; 9: 81-98.
- [6] D. Lesselier, A. Razek, Eddy current scattering and inverse scattering: Green's integral and variational formulations, in *Scattering: Scattering and Inverse Scattering in Pure and Applied Science. Part I. Scattering of Waves by Macroscopic Targets* ed R Pike and P C Sabatier (London: Academic Press) pp 486–507, 2002.